Article

Transcription Profile Analysis of Chlorophyll Biosynthesis in Leaves of Wild-Type and Chlorophyll *b*-Deficient Rice (*Oryza sativa* L.)

Minh Khiem Nguyen [1,2,3,4], Tin-Han Shih [2], Szu-Hsien Lin [2], Jun-Wei Lin [2], Hoang Chinh Nguyen [4], Zhi-Wei Yang [5,*] and Chi-Ming Yang [1,2,*]

1   Biodiversity Program, Taiwan International Graduate Program, Biodiversity Research Center, Academia Sinica and National Taiwan Normal University, Taipei 115, Taiwan; nguyenminhkhiem@tdtu.edu.vn
2   Biodiversity Research Center, Academia Sinica, Taipei 115, Taiwan; damnos@gmail.com (T.-H.S.); su043@yahoo.com.tw (S.-H.L.); edward801029@hotmail.com (J.-W.L.)
3   Department of Life Science, National Taiwan Normal University, Taipei 116, Taiwan
4   Faculty of Applied Sciences, Ton Duc Thang University, Ho Chi Minh City 700000, Vietnam; nguyenhoangchinh@tdtu.edu.vn
5   Taoyuan District Agricultural Research and Extension Station, Council of Agriculture, Taoyuan 327, Taiwan
*   Correspondence: zwyang@tydais.gov.tw (Z.-W.Y.); cmyang@gate.sinica.edu.tw (C.-M.Y.)

Abstract: Photosynthesis is an essential biological process and a key approach for raising crop yield. However, photosynthesis in rice is not fully investigated. This study reported the photosynthetic properties and transcriptomic profiles of chlorophyll (Chl) *b*-deficient mutant (*ch11*) and wild-type rice (*Oryza sativa* L.). Chl *b*-deficient rice revealed irregular chloroplast development (indistinct membranes, loss of starch granules, thinner grana, and numerous plastoglobuli). Next-generation sequencing approach application revealed that the differential expressed genes were related to photosynthesis machinery, Chl-biosynthesis, and degradation pathway in *ch11*. Two genes encoding PsbR (PSII core protein), *FtsZ1*, and *PetH* genes, were found to be down-regulated. The expression of the *FtsZ1* and *PetH* genes resulted in disrupted chloroplast cell division and electron flow, respectively, consequently reducing Chl accumulation and the photosynthetic capacity of Chl *b*-deficient rice. Furthermore, this study found the up-regulated expression of the *GluRS* gene, whereas the *POR* gene was down-regulated in the Chl biosynthesis and degradation pathways. The results obtained from RT-qPCR analyses were generally consistent with those of transcription analysis, with the exception of the finding that *MgCH* genes were up-regulated which enhance the important intermediate products in the Mg branch of Chl biosynthesis. These results indicate a reduction in the accumulation of both Chl *a* and Chl *b*. This study suggested that a decline in Chl accumulation is caused by irregular chloroplast formation and down-regulation of *POR* genes; and Chl *b* might be degraded via the pheophorbide *b* pathway, which requires further elucidation.

Keywords: Chl *b*-deficient mutant; photosynthesis; RNA-Seq transcriptome

1. Introduction

Rice (*Oryza sativa* L.) is a major staple food supplying to 50% population worldwide [1]. Its production has recently increased to meet the growing demands for a rapid increase in world population. However, the rice yield is significantly affected by many factors including variety, climate, terrain, temperature, light intensity, soil properties, and polluted farmland, which are related to its development and photosynthetic capacity [2–5]. Therefore, there is an urgent need to investigate photosynthesis in rice under different environmental conditions.

Photosynthesis is an essential biological process in higher plants, which contributes to approximately 90% of biomass production in crops. Consequently, enhancing photosyn-

thesis could be an effective strategy for elevating crop yield [6–8]. Chlorophylls (Chls) are photosynthetic pigments, which include Chl *a* and Chl *b*. They are essential components of the plant photosystems, which are used to absorb and transfer light energy [9–11]. Even though Chl *a* along with Chl *b* and carotenoid (Car) are found throughout higher plants, extremely different Chl *a/b* ratios have been reported in many mutant plants [12–14]. Chl *b* differs from Chl *a* in structure only in the presence of a formyl group instead of a methyl group at C-7 position [15]. This change in structure results in different wavelength absorptions, as Chl *a* absorbs red-blue light, whereas Chl *b* absorbs blue and orange light [16–18]. Thus, Chl *a/b* affects photosynthesis capability in plant [19]. Moreover, numerous studies on rice have shown that an increase in Chl content (i.e., Chl *a*, Chl *b*, and total Chl) significantly enhances the rice yield [10,20]. However, studies on its mechanism (photosynthetic machinery biogenesis) are still limited. Therefore, a deeper understanding of Chl biosynthesis and degradation may provide an effective approach for enhancing biomass production and crop yield [21–23].

Chl biosynthesis and degradation pathway are composed of four distinct sections: (1) the common pathway, (2) Mg branch, (3) Chl cycle, and (4) Chl degradation pathway. The common pathway includes nine enzymatic reactions to convert L-glutamate into protoporphyrin IX. The enzymes involved in this pathway are glutamyl-tRNA synthetase (*GLuRS*), glu-tRNA reductase (*GluTR*), glutamate 1-semialdehyde aminotransferase (*GSA-AT*), porphobilinogen synthase (*ALAD*), hydroxymethylbilane synthase (*PBGD*), uroporphyrinogen decarboxylase (*UROD*), coproporphyrinogen III oxidase (*CPOX*), and protoporphyrinogen oxidase (*PPOX*). In the Mg branch, five enzyme-catalyzed reactions are carried out to convert protoporphyrin IX into divinyl chlorophyllide *a* using Mg-chelatase (*MgCH*), Mg-protoporphyrin IX methyltransferase (*MgMT*), Mg-protoporphyrin IX monomethyl ester cyclase (*MPEC*), protochlorophyllide reductase (*POR*), and 3,4- divinyl protochlorophyllide *a* 9-vinyl reductase (*DVR*) as a catalyst. The Chl cycle includes the interconversion of Chl *a* and Chl *b*, which is catalyzed by chlorophyllide *a* oxygenase (*CAO*), chlorophyll synthase (*CHLG*), chlorophyll *b* reductase (*NOL*), and 7-hydroxymethyl chlorophyll *a* reductase (*HCAR*). In the final section (the Chl degradation pathway), Chl *a* is degraded to form the non-fluorescent Chl catabolite (NCC) through five reactions, which are respectively catalyzed by chlorophyllase (*CHL*), magnesium dechelatase (*MCS*), pheophorbide *a* oxygenase (*PAO*), and red chlorophyll catabolite reductase (*RCCR*) [24–26].

Chloroplast is a unique organelle in higher plants where photosynthesis occurs. Its development has an impact on plant growth due to its role in supplying energy, amino acids, and lipids, as well as another important metabolism process [27]. The most important structure in chloroplast is thylakoid, which contains Chl *b* and serves as the platform for photosynthesis's light reactions. Therefore, impairing chloroplast development may influence the photosynthetic capacity and leaf development [28].

Mutagenesis has proven to be a valuable approach for studying pigment synthesis in higher plants, with a number of corresponding mutants having been identified [29–31]. Chl-deficient mutants have been used to study the Chl biosynthesis pathway and photosynthetic machinery biogenesis in barley, maize, pea, wheat, rice, soybean, and sweet potato [32–38]. Chl-deficient mutants can generally be classified into two main types, namely, Chl *b*-lacking mutants (with undetectable Chl *b*) and Chl *b*-deficient mutants (containing reduced levels of Chl *b*) [39]. Particularly, the wild-type Norin No.8 rice is treated with ionizing radiation and various mutagenic chemicals to obtain a collection of Chl *b*-deficient mutant rice [40–42]. Several of them have been used to study the photosynthesis in rice. Recently, Nguyen et al. [26] has reported the photosynthetic characteristics and transcription profiles of Chl *b*-lacking mutant rice (mutant rice type 1). However, the Chl biosynthesis and degradation underlying different Chl *a/b* ratios in rice still remains unclear. Therefore, further studies on other rice mutants are still required to clarify the Chl biogenesis. To address this concern, Chl *b*-deficient mutant (mutant rice type 2) is proposed as a potential and valuable resource for studying the photosynthesis pathway

in rice. However, the transcription profiles and photosynthetic characteristics of the Chl *b*-deficient mutant rice have not yet been reported.

In this study, next-generation sequencing (NGS) was used to determine the transcription profiles and photosynthetic characteristics of Chl *b*-deficient mutant rice type 2a (Chl *a/b* of ~10). The characteristics, differentially expressed genes (DEGs), and transcription factors (TFs) related to Chl biosynthesis and degradation in wild-type and the Chl *b*-deficient rice type 2a were compared.

2. Materials and Methods

2.1. Plant Materials and Growth Condition

Seeds of wild-type (Norin No. 8, *wt*) and Chl *b*-deficient mutant rice type 2a (chlorina 11, *ch11*) were kindly provided by Dr. Tomio Terao (Department of Applied Physiology, National Institute of Agrobiological Resources, Tsukuba Science City, Japan). The seeds were sown in a growth chamber (Firstek Scientific Co Ltd., New Taipei, Taiwan), and the germinated seedling was subsequently grown for 6 weeks at a temperature of 25 °C, and relative humidity of ≥80%, under a 12/12 dark cycle at Biodiversity Research Center, Academia Sinica Institute, Taipei, Taiwan (25°02′34.1″ N, 121°36′40.7″ E). The leaves of these plants were then harvested, immediately frozen in liquid nitrogen, and stored at −80 °C for less than 2 weeks for further analysis.

2.2. Assessment of Pigment Contents

Approximately 0.1 g of wild-type and mutant leaf tissues were cut into pieces, immersed in 1 mL acetone (80%, *v/v*) at 4 °C, and homogenized using bullet blender tissue homogenizer (Next Advance Inc., New York, NY, USA) for 5 min. The extracts were then obtained through filtration. The absorption of the extracts was measured at 663.6, 646.6, and 440.5 nm using a Hitachi U2800 UV-Visible spectrophotometer (Hitachi, Tokyo, Japan) at room temperature to determine pigment contents (total Chl, Chl *a*, Chl *b*, and carotenoids (Car)) according to the method described by Yang et al. 1998. The pigment contents were calculated (on the basis of μg/mL Chl/g fresh weight [43]), as follows:

$$\text{Chl } a = 12.25A_{663.6} - 2.55A_{646.6} \tag{1}$$

$$\text{Chl } b = 20.31A_{646.6} - 4.91A_{663.6} \tag{2}$$

$$\text{Total Chl} = 17.76A_{646.6} + 7.34A_{663.6} \tag{3}$$

$$\text{Car} = 4.69A_{440.5} - 4.91 \text{ Total Chl} \tag{4}$$

where Chl *a*, Chl *b*, and total Chl are the Chl *a*, Chl *b*, and total Chl content, respectively; $A_{646.6}$, $A_{646.6}$, $A_{440.5}$ are the absorbance of the extracts which was measured at 663.6, 646.6, and 440.5 nm, respectively.

To validate the Chl content, soil–plant analysis development (SPAD) values were determined in situ on *wt* and *ch11* plants using a SPAD-502Plus chlorophyll meter (Konica Minolta, Osaka, Japan).

2.3. Ultrastructure Microscope

Wild-type and mutant leaf tissues were cut into small sections (approximately 0.5 × 0.5 × 0.5 mm³ in size) and immersed in 2.5% glutaraldehyde at 4 °C for 24 h, followed by 1% OsO₄ for 2 h. Thereafter, the tissues were cut into 70 nm thin sections using a Leica EM UC6 ultramicrotome (Leica Microsystems GmbH, Wetzlar, Germany), stained with 1% (*w/v*) uranyl acetate (20 min) and 1% (*w/v*) lead citrate (5 min) [44], and then visualized using a Phillip Tecnai 12 transmission electron microscope (JEOL Ltd., Tokyo, Japan) for ultrastructural observations.

2.4. cDNA Libraries Construction and Transcriptome Sequencing

Total RNA was extracted from the whole leaves of *wt* and *ch11* rice using a RNeasy Plant Mini Kit (Qiagen, Hilden, Germany), following the manufacturer's instructions. The purity and quantity of RNA samples were evaluated using 1% formaldehyde agarose gel electrophoresis and determined with a NanoDropTM 2000 spectrophotometer (NanoDrop, Wilmington, NC, USA). RNA concentration and integrity were determined using an Agilent 2100 Bio-analyzer (Agilent RNA 6000 Nano Kit; Agilent Technologies, Inc., Santa Clara, CA, USA). Briefly, two sets of paired-end cDNA libraries were constructed from each wild-type and mutant rice sample, and the resulting cDNA libraries were sequenced using the BGISEQ-500 platform (Beijing Genomics Institute, Shenzhen, Guangdong, China) for transcriptome sequencing. As the result, the total raw reads of *wt* (30.60, 30.61 Mb) and *ch11* (30.62, 30.63 Mb) were generated. Adapter sequences, unknown nucleotides, and low-quality sequences were removed using SOAPnuke v1.5.2 (https://github.com/BGI-flexlab/SOAPnuke, accessed on 12 March 2021). Both cDNA library construction and transcriptome sequencing were conducted independently by a commercial service provider (Tri-I Biotech, Inc., The New Taipei City, Taiwan). Two biological replications of each sample in RNA-Seq were used to conduct a library.

2.5. Transcriptome Analysis

The clean reads were mapped to the *Oryza sativa* 'Nipponbare' reference genome (http://rapdb.dna.affrc.go.jp/, accessed on 12 March 2021) based on hierarchical indexing for the spliced alignment of transcripts in HISAT (Hierarchical Indexing for Spliced Alignment of Transcripts) using HISAT2 v2.0.4, (http://www.ccb.jhu.edu/software/hisat, accessed on 12 March 2021). The clean reads were mapped to the reference using Bowtie2 v2.2.5, (http://bowtie-bio.sourceforge.net/ Bowtie2 /index.shtml, accessed on 12 March 2021), and we then calculated gene expression levels using RSEM v1.2.12, (http://deweylab.biostat.wisc.edu/RSEM, accessed on 12 March 2021). Pearson correlation, hierarchical clustering analyses, and generation of the sample were performed using the cor, hclust, and ggplot2 functions of R, respectively. Furthermore, DEGs were detected using PossionDis, which is based on Poisson distribution with default parameters of a fold change ≥ 2.00 and FDR ≤ 0.001 [45], and subsequently subjected to Gene Ontology (GO) and KEGG pathway analyses for determinations of functional enrichment using the phyper function of R.

2.6. Quantitative RT-qPCR

Quantitative RT-qPCR was performed to validate and analyze the basic expression levels of a subset of candidate genes involved in Chl biosynthesis and degradation pathways. Total RNA (µg) isolated from the leaves of wild-type and mutant plants was used to synthesize cDNA using a Transcriptor First Strand cDNA Synthesis Kit (Roche Diagnostic Systems, Branchburg, NJ, USA) and oligo (dT) primers. The sequences of primer sets used for amplification were designed using Primer Premiere 6 software (Premiere Biosoft, Palo Alto, Santa Clara, CA, USA) (Table S1, Supplementary Materials). RT-qPCR was performed using the StepOne Plus Real-Time PCR system (Applied Biosystems, Life Technologies Inc., Foster City, CA, USA) with Roche FastStar Universal SYBR Green Master reagent (Roche Diagnostic Systems, Branchburg, NJ, USA). Relative gene expression values were calculated using $2^{-\Delta\Delta Ct}$ comparative Ct method [46].

2.7. Statistical Analysis

The pigment contents, SPAD values, and relative gene expression (RT-qPCR results) of wild-type and mutant rice were statistically analyzed by the least significant difference (LSD) *t*-test at a *p* value ≤ 0.05, which was performed using the SAS v8.0 statistical package (SAS Institute, Cary, NC, USA).

3. Results

3.1. Characterization of ch11 Rice

Seeds of *wt* and *ch11* rice were grown in a growth chamber for 6 weeks under controlled conditions (25 °C, 12/12 dark cycle, RH ≥ 70%). After the cultivation, *ch11* plantlets showed dwarf and unhealthy phenotypes (~25 cm in height) with green leaves, whereas *wt* plantlets showed normal and healthy development (~40 cm in height) with dark green leaves (Figure 1a,b). The total Chl content of *wt* (3.3 mg g^{-1}) was almost twice that of the *ch11* (1.7 mg g^{-1}). A similar difference was detected for carotenoid (Car) content (0.5 and 0.3 mg g^{-1} for *wt* and *ch11*, respectively). Moreover, the content of Chl *a* in *ch11* was approximate 64% that in the *wt*, whereas that of Chl *b* was only approximately 12.5%. Consequently, the *ch11* mutant was characterized by a notably high Chl *a*/*b* of 11.25, which was almost three times higher than that of *wt* leaves (Figure 1c). Furthermore, soil–plant analysis development (SPAD) values were determined to validate the Chl accumulation in the leaves of *wt* and *ch11* plants, obtaining values, 29.62 and 16.23, respectively. This result was consistent with our Chl assessments and indicative of abnormal Chl biosynthesis and degradation in Chl *b*-deficient rice. Differences were also observed with respect to the ultrastructure of *wt* and *ch11* leaves, with the leaves of *wt* plants being characterized by healthy chloroplasts with distinct membranes, and stromal lamellae, small starch granules, and few plastoglobuli (Figure 2a). In contrast, the chloroplasts in *ch11* leaves showed abnormal development with indistinct membranes, indistinct or absent stromal lamellae, no starch granules, and numerous plastoglobuli (Figure 2b. Moreover, although stacked thylakoid grana were observed clearly in *ch11* leaf sections, they were some two to five times thinner than the stacked grana in *wt* chloroplasts (Figure 2a,b).
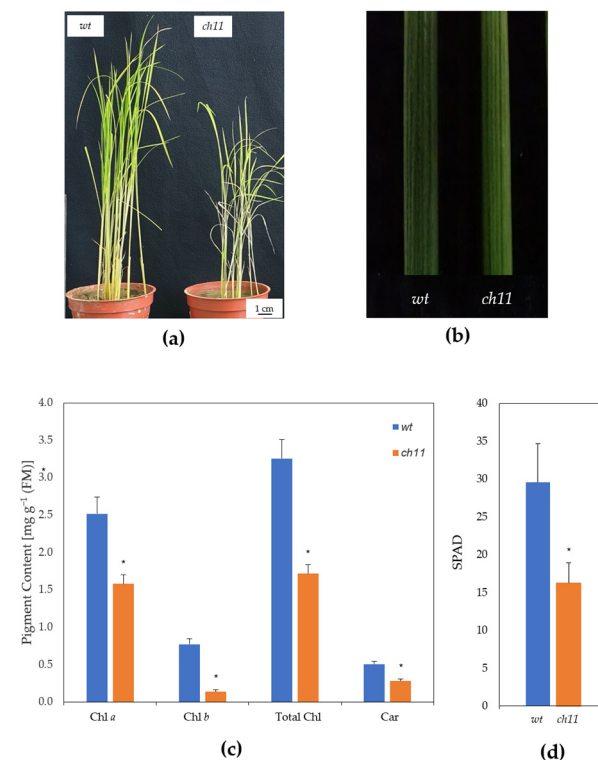

(a)   **(b)**

(c)   **(d)**

Figure 1. Plantlet phenotypes and assessments of leaf coloration and pigment contents. (**a**) Phenotypes of wild-type (*wt*) and chlorophyll *b*-deficient (*ch11*) rice; (**b**) Leaf coloration of *wt* and *ch11* rice; (**c**) Chlorophyll (Chl) and carotenoid (Car) contents of *wt* and *ch11* rice; (**d**) Soil–plant analysis development (SPAD) values of *wt* and *ch11* rice. Asterisks (*) indicate significant differences between the pigment contents of the *wt* and *ch11* rice ($p \leq 0.05$).
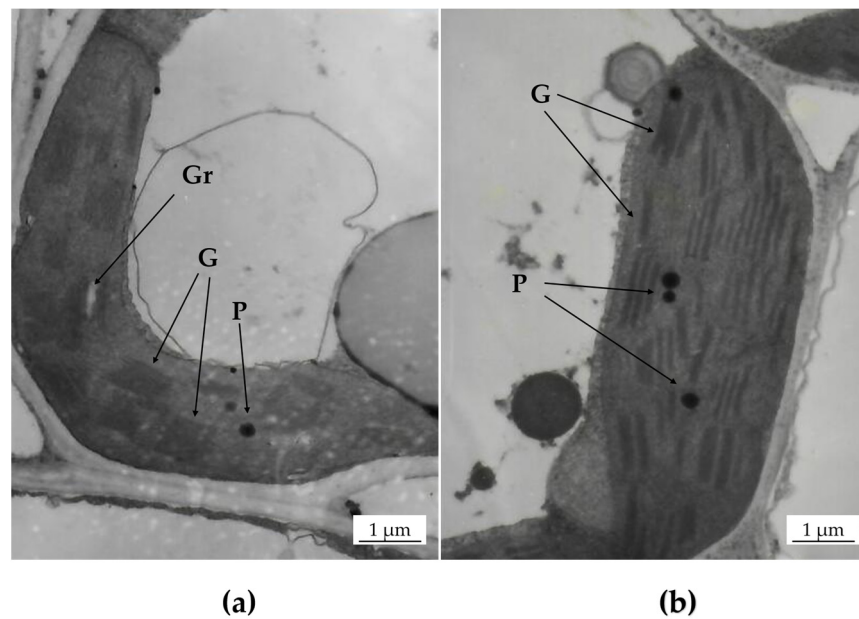
(a)   **(b)**

Figure 2. Chloroplast ultrastructure of wild-type (*wt*) and chlorophyll *b*-deficient (*ch11*) rice. (**a**) Normal chloroplast structure of *wt* rice; (**b**) Abnormal chloroplast structure of *ch11* rice, showing indistinct thylakoid membranes, an absence of granules, and numerous plastoglobuli. G, grana; P, plastoglobuli; Gr, granules.

3.2. Genome Mapping and Gene Expression Analysis

In this study, we sequenced samples from *wt* and *ch11* seedlings using the BGISEQ-500 platform. The obtained raw sequencing reads were filtered by removing low-quality reads, adaptor sequences, and reads with a high content of unknown bases. The resulting 25.31–29.33 million clean reads were subsequently mapped to the rice reference genome (*Oryza sativa* 'Nipponbare', http://rapdb.dna.affrc.go.jp/, accessed on 12 March 2021) using HISAT (hierarchical indexing for spliced alignment of transcript), with match ratios in the range of 96.84–97.93% (Table S2, Supplementary Materials). Among the sequences in the *wt* and *ch11* libraries, 88.93% and 89.67%, were respectively mapped to the reference transcript, and 79.56% and 80.42% of the uniquely mapped reads were mapped to a single locus in the reference genome (Table S3, Supplementary Materials). Approximately 91.41% of the expressed genes were shared between *wt* and *ch11* rice genome (Figure 3).
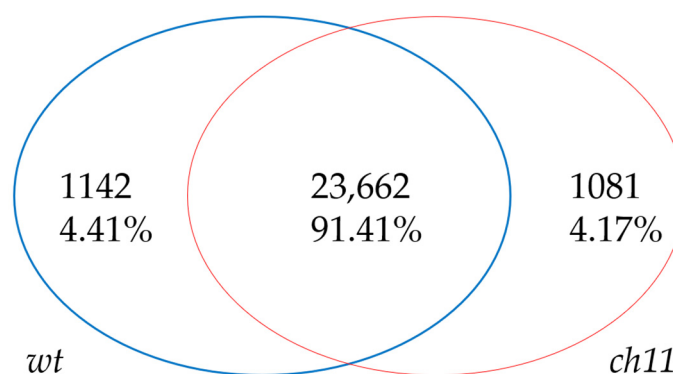

Figure 3. Comparison of gene expression in wild-type (*wt*) and chlorophyll *b*-deficient (*ch11*) rices.

3.3. Detection and Annotation of Differentially Expressed Genes

Functional annotation was conducted to acquire information with respect to protein function, pathway involvement, and GO. Sequence orientation-driven genes were aligned based on the KEGG database. GO is a global criteria functional identification scheme for

genes in which biological processes, cellular components, and molecular functions are assigned to transcripts. The distribution of detected genes among the GO categories is shown in Figure 4. A total of 5510 genes were mapped, with 1992, 2325, and 1193 genes being assigned to "Biological Process", "Cellular Component", and "Molecular Function", respectively. Notably, individual genes can be assigned to multiple GO terms. DEGs were identified using the fragments per kb per million reads method, and Poisson distribution, with false discovery rate (FDR) $\leq$ 0.001 and absolute log2 ratio $\leq$ 1 (Figure 5a,b). We accordingly identified 863 and 2007 DEGs, which were up- and down-regulated, respectively, in *ch11* leaves, whereas 23,015 genes showed no significant differences in expression between *wt* and *ch11* leaves (Figure 5b).
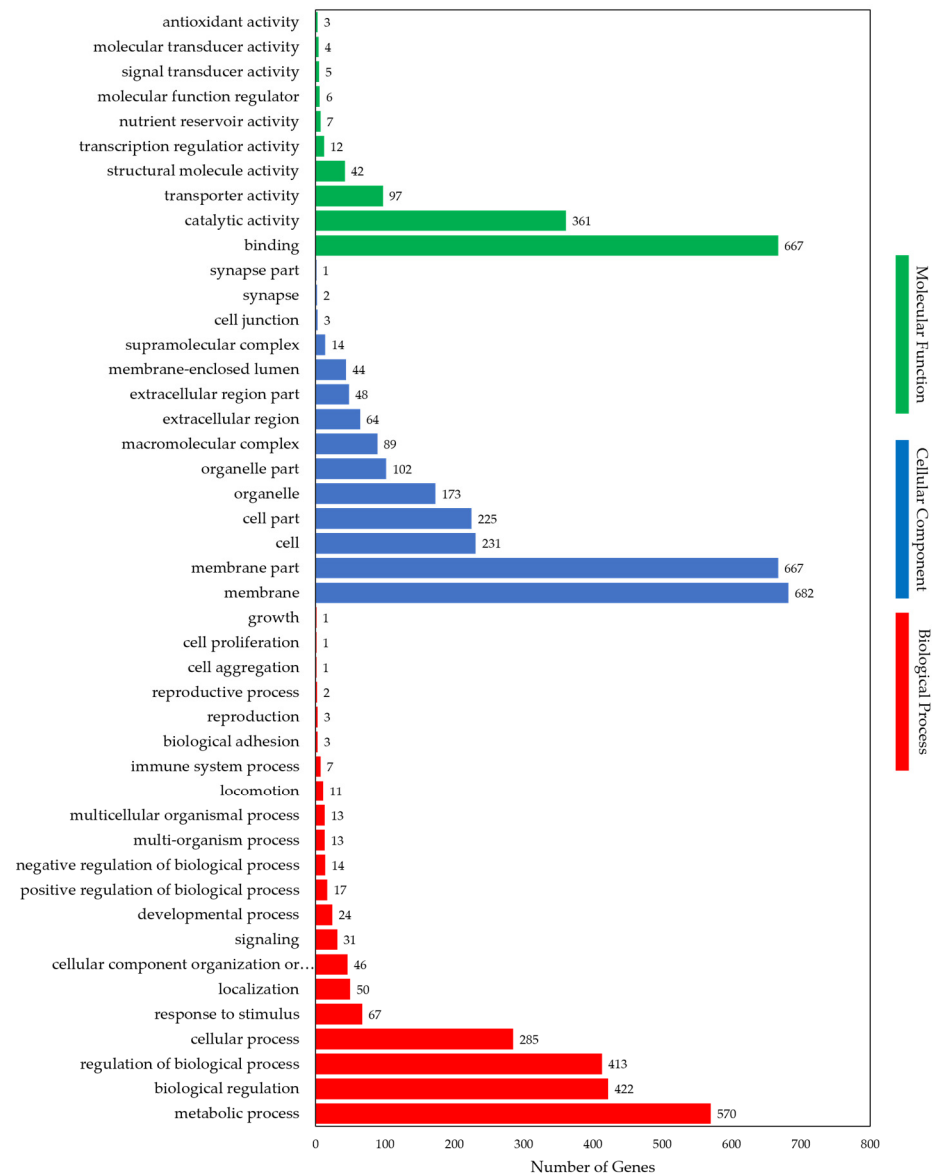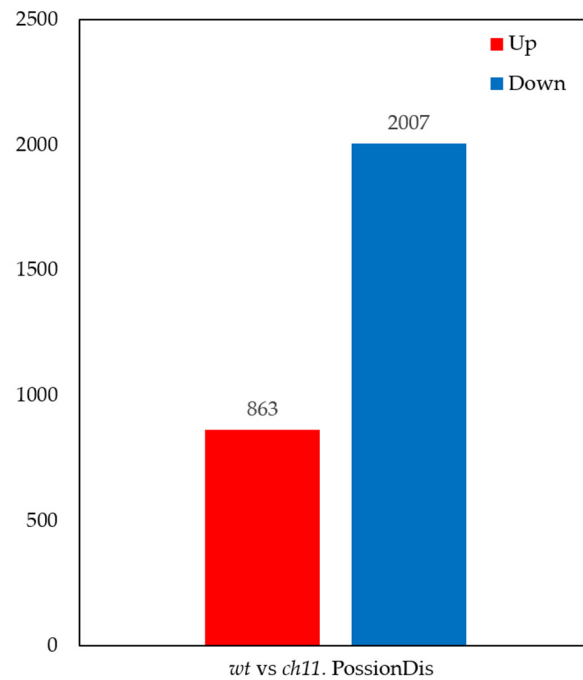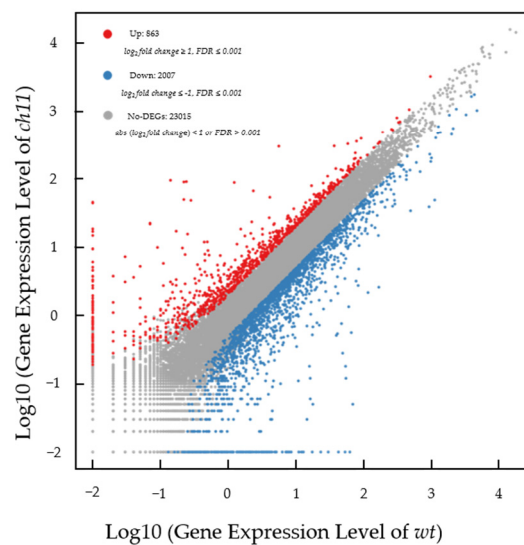

Figure 4. Gene Ontology classification of differentially expressed genes in wild-type and chlorophyll *b*-deficient rice.

(a)

(b)

Figure 5. Differentially expressed genes (DEGs) in wild-type (*wt*) and chlorophyll *b*-deficient (*ch11*) rice. (**a**) Comparison of up- and down-regulated DEGs; (**b**) Classification of genes, based on differences in expression level.

3.4. Role of Chlorophyll Metabolism Genes in Leaf Coloration

DEGs related to chloroplast development and cell division were identified based on KEGG pathway annotation. Genes related to the *FtsZ1* cell division-related protein gene (Osa_4333567) and two *PsbR* chloroplast photosystem II protein genes (Osa_107276047 and Osa_4342395) were found to be down-regulated in *ch11* rice (by 2.1, 1.7, and 4.5-fold, respectively). Furthermore, the *PetH* gene (Osa_4334338) and *Lhcb1* gene (Osa_4324705) encoding an FDX electron transfer protein and photosynthesis-antenna protein, respectively, was also down-regulated (Table 1). A total of 24 DEGs related to Chl biosynthesis and five

DEGs related to Chl degradation were identified based on KEGG pathway annotation. The expression levels of the DEGs were determined using hierarchical cluster analysis (Figure 6). *GLuRS* (Osa_4338118), and *NCCR* (Osa_4348519) were significantly up-regulated in *ch11* (Δlog2 = 1.4, and 1.7, respectively), whereas *POR* (Osa_4337415) was down-regulated (−1.7) compared with the *wt* (Figure 6). These results indicate that the processes of Chl biosynthesis and degradation may be detrimentally affected in the *ch11* mutant.

Table 1. Distribution of unigenes amongst KEGG pathways containing differentially expressed genes.

Function	Gene ID	TF Family	Log2 Fold Change	Expression in *ch11* Compared to *wt*	Annotation
Chlorophyll biosynthesis	*Osa_4328118*	*GLuRS*	1.4	Up-regulated	glutamyl-tRNA synthetase
	Osa_4337415	*POR*	−1.7	Down-regulated	protochlorophyllide reductase A
	Osa_4348519	*NCCR*	1.7	Up-regulated	Red chlorophyll catabolite reductase
Photosynthesis	*Osa_107276047*	*PsbR*	−1.7	Down-regulated	photosystem II 10 kDa protein
	Osa_4342395	*PsbR*	−4.5	Down-regulated	photosystem II 10 kDa protein
	Osa_4334338	*PetH*	−1.1	Down-regulated	ferredoxin-NADP+ reductase
Antenna protein	*Osa_4324705*	*Lhcb1*	−1.7	Down-regulated	Photosynthesis-antenna protein
Chloroplast division	*Osa_4333567*	*FtsZ1*	−2.1	Down-regulated	Cell division protein FtsZ homolog 2-1

TF, transcription factor; *ch11*, chlorophyll *b*-deficient mutant of rice (Chlorina 11).
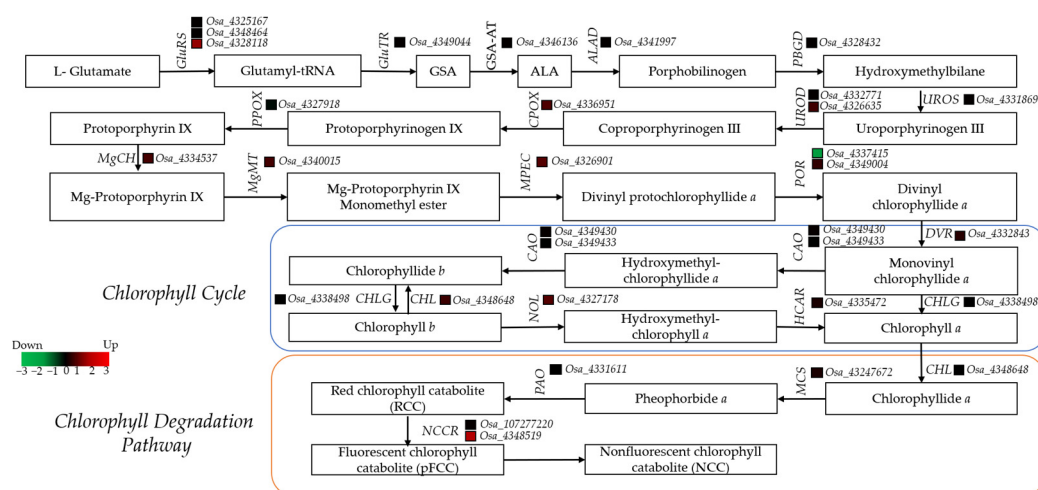

Figure 6. Expression profiles of differentially expressed genes (DEGs) involved in chlorophyll (Chl) biosynthesis and degradation. The expression levels of the Chl *b*-deficient (*ch11*) are compared with those of wild-type (*wt*) rice.

3.5. Role of Transcription Factors in Leaf Coloration

TFs are key regulatory proteins that play important roles in the regulation of gene expression. In the present study, 289 DEGs were identified as putative TFs and were found to be associated with a total of 39 TF families. The most well represented TF family was the MYB superfamily (42 DEGs), followed by the bHLH (34), MYB-related (32), NAC (28), WRKY (26), and AP2-EREBP (13) families (Table 2). In *ch11* rice, 38, 28, 29, 27, and 12 DEGs in the MYB, MYB-related, bHLH, NAC, WRKY, and AP2-EREBP families, respectively, were found to be down-regulated. Similarly, we detected 13, 12, 9, 8, 8, and 6 DEGs in the AP2-EREBP, MADs, ARF, G2-like, GRAS, and C2H2 TF families, respectively. Most of these genes were significantly down-regulated in *ch11* rice. Moreover, 2 DEGs were associated with the FAR1 and mTERF TF families, respectively, which were down-regulated in *ch11* (Table 2).

Table 2. Summary of differentially expressed transcription factor genes in chlorophyll *b*-deficient (*ch11*) rice compared with wild-type rice.

Transcription Factor Family	Total No. Genes	No. Genes Up-Regulated	No. Genes Down-Regulated
ABI3VP1	1	0	1
Afin-like	1	1	0
AP2-EREBP	13	1	12
ARF	5	0	5
ARR-B	4	0	4
BBR/BPC	2	2	0
bHLH	34	5	29
bZIP	4	0	4
C2C2-Dof	6	0	6
C2C2-GATA	1	0	1
C2C2-YABBY	4	0	4
C2H2	6	0	6
C3H	1	0	1
CSD	1	0	1
E2F-DP	2	0	2
FAR1	14	12	2
G2-like	8	0	8
GRAS	8	1	7
GRF	4	1	3
HB	1	0	1
HSF	1	0	1
LIM	1	0	1
LOB	1	0	1
MADS	12	2	10
mTERF	5	3	2
MYB	42	4	38
MYB-related	32	4	28
NAC	28	1	27
OFP	1	0	1
PBF-2-like	1	1	0
SBP	1	0	1
Sigma70-like	2	2	0
SRS	2	0	2
TCP	2	2	0
Tify	6	0	6
Trihelix	2	0	2
TUB	1	0	1
WRKY	26	4	22
zf-HD	2	1	1

3.6. RT-qPCR Validation of Differentially Expressed Chlorophyll Biosynthesis Genes

RT-qPCR expression analyses were performed to validate the identification of DEGs related to Chl biosynthesis and degradation. The expression patterns of 12 genes that code enzymes involving in 19 reactions in Chl biosynthesis were examined. The result revealed that these genes were similar to those observed in the RNA-Seq data (Figure 7). The RT-qPCR results were generally consistent with the transcription analysis data, with the exception of one gene (*MgCH*) showing an inconsistent expression pattern. *POR* was observed to be markedly down-regulated in *ch11*, whereas most of the genes showed non-significant changes. In contrast to the transcription analysis results, the qPCR results revealed that *MgCH* was up-regulated in *ch11* (Figure 7).
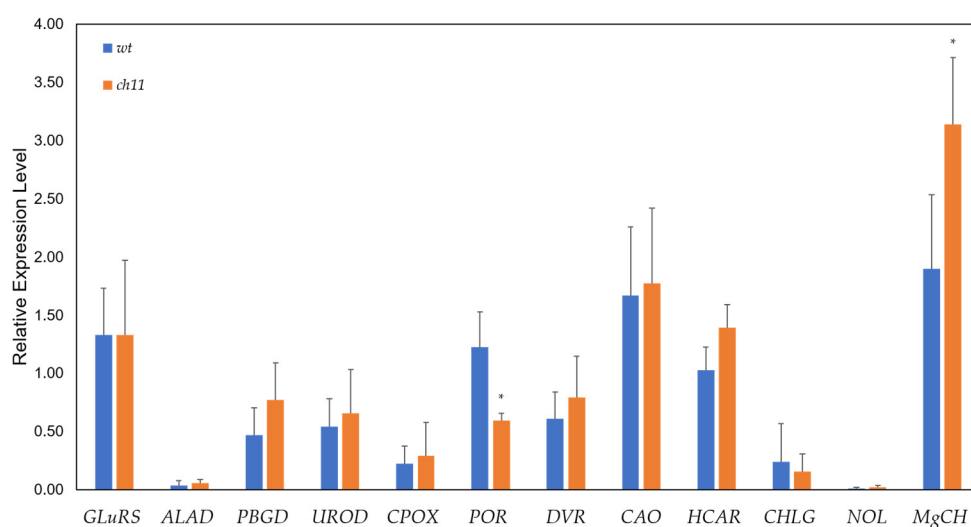
Figure 7. Expression of levels of 12 differentially expressed genes from wild-type (*wt*) and chlorophyll *b*-deficient (*ch11*) rice. Gene expression was measured using quantitative RT-qPCR. Asterisks (*) indicate significant differences between the expression levels of the wild-type and *ch11* rice ($p \leq 0.05$).

4. Discussion

4.1. Pigment Contents and Chloroplast Development

Chl-deficient mutants have been widely used to study Chl biosynthesis and the photosynthetic machinery properties of barley, maize, pea, sweet clover, wheat, rice, soybean, sugar beet, and the maiden-hair tree [32–34,47,48]. At the physiological level, pigment contents, the Chl *a*/*b*, and chloroplast development are associated with the coloring of the leaves in higher plants [49]. Accordingly, differences in leaf coloration have been observed between Chl-deficient mutants and the corresponding wild-type plants in species such as *Arabidopsis thaliana*, *Gingko biloba*, and *Oryza sativa*. Previous studies have identified two types of Chl-deficient rice mutant, which are based on the ratio of Chl *a* to Chl *b*, namely, type 1, in which Chl *b* is completely absent (Chl *b*-lacking mutants), and type 2, characterized by high Chl *a*/*b* ratios of between approximately −10 and −15 (Chl *b*-deficient mutant) [41,42,50]. Moreover, a study indicated that the Chl *a*/*b* in *ch11* slightly fluctuated from 9 to 11 in 6 days incubation in various irradiances [50]. In our previous study, we observed reductions in Chl content, an absence of Chl *b*, and abnormal chloroplast development in Chl *b*-lacking mutants, which were characterized by light green leaves compared with the dark green pigmentation seen in the leaves of wild-type plants [26]. In the present study, we also noted visible differences in the leaf coloration of Chl *b*-deficient mutant and wild-type rice, with leaves of the mutant being a distinctly paler green compared with the dark green of the wild-type leaves. In addition, mutant plants showed a dwarf phenotype, together with marked reductions in the contents of total Chl and Chl *b* in leaves, as indicated Chl *a*/*b* of up to approximately 11.5, compared with the wild-type. Thus, we can assume that differences in Chl content and Chl *a*/*b* between the Chl *b*-deficient mutant and wild-type rice contributed to the observed variation in leaf coloration. Moreover, the presence of Chl *b* in *ch11*, albeit at a lower level, would account for the darker coloration compared with the light-green leaves characterizing Chl *b*-lacking mutant [26]. Given that the processes of photosynthesis and Chl biosynthesis occur in chloroplasts, organelles unique to higher plants [51,52], abnormal development in these structures can be expected to have a detrimental influence on the photosynthetic capacity and Chl synthesis of leaves [26,53]. Numerous studies have reported irregular chloroplast development (i.e., indistinct thylakoid membrane, non-existent granules, abundant vesicle, and numerous plastoglobuli) in Chl-deficient mutants, including those of green bamboo, maidenhair tree, and rice, which affects Chl contents, Chl *a*/*b*, and leaf coloration, compared with the corresponding wild-type [26,54,55]. Moreover, the integrity of the stacked

grana of chloroplasts determines the efficiency of light absorption and energy conversion in the photosynthetic apparatus [56]. In this study, the chloroplast ultrastructure analysis revealed that *wt* rice was characterized by normally developed chloroplasts containing an abundance of thick stacked grana, whereas *ch11* leaves showed distinctly abnormal chloroplast development (i.e., indistinct thylakoid membranes, numerous plastoglobuli, and absence of starch granules) with abundant thinner stacked grana. These observations indicate that in conjunction with a lower Chl content, irregular chloroplast development would contribute to deficiencies in the harvesting and conversion of light energy in *ch11* compared with *wt* rice. A similar pattern has been observed in the leaves of Chl *b*-lacking rice (*ch1*), in which abnormal chloroplast development along with thinner grana was found to be associated with a reduction in pigmentation, an elevated Chl *a/b*, and reduced photosynthetic capacity [26]. Accordingly, at the physiological level, the dwarf phenotype and leaf color variation of the Chl-deficient rice are believed to be closely associated with a reduced Chl content, higher Chl *a/b*, and abnormal chloroplast development, which are presumed to contribute to a reduced photosynthetic capacity and thus have detrimental effects on the biomass and yield of rice.

4.2. Chloroplast-Related Differentially Expressed Genes and Photosynthetic Capacity

Next-generation sequencing and transcriptome profiling can provide valuable information regarding those genes that are differentially expressed between different interested genotypes [57,58]. In the present study, transcriptome profiling of *wt* and *ch11* rice revealed a total of 863 and 2007 DEGs being up- and down-regulated, respectively. Among them, we identified a number of genes associated with photosynthetic machinery, chloroplast development, and pigment biosynthesis metabolism that may be associated with the observed differences in Chl *a/b*. The coordination of plastid and nuclear genes in plants plays an important role in normal chloroplast development. Differences in the levels of chloroplast-related gene expression could affect the biogenesis of chloroplast assembly and pigment contents, thus resulting in changes in Chl accumulation, Chl *a/b*, photosynthetic capacity, and leaf coloration [54,59]. In this regard, *FtsZ1* and *FtsZ2* in the FtsZ family of protein are key players in the initiation and progression of chloroplast division in plants and green algae [60,61]. The analysis of chloroplast-related DEGs, revealed a downregulated expression of the *FtsZ1* gene in *ch11* rice, indicating a potential deficiency in chloroplast cell division compared with the *wt*. This result is consistent with the abnormal chloroplast development and leaf color variation characterizing *ch11* rice. The chloroplast abnormalities observed in the *ch11* mutant are thus assumed to result in a reduction in Chl *b* content and a concomitant increase in the Chl *a/b*. In higher plants, the light-harvesting complex (or antenna complex, LHC) proteins play an important role in the photosynthetic apparatus, which absorbs and regulates the flow of light energy to photosystems I (PSI) and II (PSII) [62,63]. PSII is a multi-protein-pigment complex that contains the PSII core reaction center dimer, LHCII, and minor light-harvesting complexes comprising more than 20 subunits, including PsbR [64,65]. Moreover, LCHII has been reported to be a key factor that regulates the stacking of grana thylakoids in chloroplasts [66–68]. Previous studies have found that a reduction in or absence of LHC proteins in Chl-deficient mutants of *Arabidopsis thaliana, Hordeum vulgare,* and *Oryza sativa* are associated impairment in stacked grana [26,69–72]. Hence, the chloroplast of Chl-deficient mutants is predicted to be characterized by the poorly developed or non-existent stacked grana [69,73]. In the present study, we found that the expression of two *PsbR* genes was also down-regulated in *ch11* rice, by 1.7- and 4.5-fold, respectively, which might be indicative of a reduction in the level of LHCII proteins, and consequently a reduction in photosynthetic capacity. A similar pattern has been detected in Chl *b*-lacking rice, in which two LHCII family *PsbR* genes were shown to be markedly down-regulation, leading to a reduced photosynthetic capacity [26]. Moreover, chloroplast FNR proteins include PetH, which plays a role in the final step of the linear flow of electrons, whereby electrons are transferred from ferredoxin to NADP$^+$ [74]. In the present study, the *PetH* gene was observed to be down-regulated

in *ch11* rice, which might cause a reduction in the transfer of electrons from ferredoxin to NADP$^+$ (Table 1). Consequently, it lowers the amounts of NADPH products available for the Calvin reaction, which might lead to the small or non-existent granules in the mutant. These findings indicated that deficiencies in the photosynthetic capacity of the Chl *b*-deficient *ch11* mutant could be related to the down-regulated expression of genes associated with PSII and photosynthetic electron transport. Furthermore, stacked grana in *ch11* were found to be thinner than those in the *wt*, indicating a loss of LCHII.

4.3. RNA-Seq Analysis and Chlorophyll-Related Differentially Expressed Genes

Chl *a* and *b* play vital roles in light absorption and energy transfer [75,76]. Chl *a* is the principal pigment in higher plants involved in light-harvesting and primary photochemical reactions, whereas Chl *b*, which is synthesized from Chl *a*, functions as an accessory pigment and is only involved in light-harvesting [18,77]. At least 28 genes encode 22 enzymes involved in Chl biosynthesis and degradation in Chl *b*-lacking rice. Changes in certain DEGs were associated with disorders in Chl metabolism and altered Chl *a/b* [26]. During the early stages of Chl biosynthesis, glutamyl-tRNA synthetase (GLuRS) regulates the δ-aminolevulinic acid (ALA), resulting in changes in the expression of GLuRS. Consequently, it could affect the synthesis of early products in the Chl biosynthetic pathway and may contribute to the development of rice plants characterized by a shorter stature and yellow leaves [52,78,79]. Moreover, protochlorophyllide (Pchllide), a key intermediate in the Chl cycle section of the Chl biosynthesis pathway [24,80], is catalyzed by protochlorophyllide reductase (POR), a light-dependent protein present in angiosperms, that reduces the double bond in the D-ring in a stereo-specific manner to yield chlorophyllide (Childe) under light condition [81–83]. In the present study, a total of 28 DEGs were detected to associate with Chl biosynthesis and degradation based on KEGG pathway annotation, among which, the *GLuRS* (Osa_4328818) homolog gene was up-regulated in *ch11* rice, whereas Osa_4325167 and Osa_4348464 showed non-significant changes. This study suspects that the expression of GluRS in *ch11* may not differ substantially from that in the *wt*. In addition, no appreciable changes in the expression of *GluTR, GSA-AT, ALAD, PBGD, UROS, UROD, CPOX,* or *PPOX* was observed. These observations indicate that the synthesis of products in the early stages of Chl biosynthesis in *ch11* rice is essentially unaffected compared to *wt* rice. These observations contrast with the changes previously observed in Chl *b*-lacking rice, in which *GluRS* was found to be down-regulated leading to an inhibition of the early products of Chl biosynthesis [26]. In the Mg branch of Chl biosynthesis, *POR* (Osa_4337415) was found to be markedly down-regulated, which might have an effect of disrupting Chlide product synthesis in the Chl cycle. This result indicates that the synthesis of Chl *a* and Chl *b* were blocked or significantly reduced in *ch11* compared with the *wt*. Contrastingly, in the Chl cycle, we detected no genes that were significantly differentially expressed in *ch11* and *wt* rice. Furthermore, our detection of Chl *b* in leaves of the *ch11* mutant indicated that Chl *b* had been normally synthesized from Chl *a*. Therefore, the enzymes CAO, CHL, NOL, HCAR, and CHLG involved in the Chl cycle had been normally translated and activated. A similar pattern has previously been observed in Chl *b*-lacking rice, with exception of the *NOL* gene, which was markedly up-regulated and may thus have promoted a rapid conversion of Chl *b* to Chl *a* [26]. In this study, the presence of Chl *b* in the leaves of *ch11* rice may reflect the fact that the expression of *NOL* in this mutant does not differ significantly from that in *wt* rice. *NOL* is unbound to light-harvesting complexes including Chl *b*, chlorophyllide *b*, pheophorbide *b*, and pheophytin *b*, and has a broad substrate specificity [84]. However, pheophytin *b* and pheophorbide *b* were not generated in chloroplast due to the specificity of Mg-dechelatase [85]. Another study stated that pheophorbide *b* is accumulated during cell death after incubating a plant, whose core antenna complex contained Chl *b,* in a dark condition [84]. Consequently, the mechanism underlying pheophorbide *b* remaining in plant cells is still poorly understood. This study suggested that the marked reduction in the Chl content of *ch11* can probably be attributed to abnormal development of chloroplasts and a significant reduction in the expression of

POR. In addition, a possible explanation for the rising of Chl *a/b* in *ch11* leaves is that Chl *b* might be degraded by an alternative degradation pathway via pheophorbide *b*, which causes the absence of Chl *b* in Chl *b*-lacking rice [26]. However, the proposed pathway remains unclear, which requires further investigations.

5. Conclusions

This study reported the photosynthetic properties and transcriptomic profile of a Chl *b*-deficient mutant rice compared with *wt* plants. The Chl *b*-deficient mutant was characterized by a dwarf phenotype along with green leaves, a reduced pigment accumulation, a high Chl *a/b*, and abnormal chloroplast structure. RNA-Seq analysis revealed that 2870 genes were differentially expressed in *ch11*. Among these genes, there were 288 TFs related to Chl biosynthesis and degradation, plastid development, cell division, and photosynthetic machinery. This study found the down-regulated expression of *POR* gene, whereas the *GluRS* gene was up-regulated in the Chl biosynthesis and degradation pathways. Changes in the expression of genes were related to chloroplast development. An increase in the Chl *a/b* may be attributed to abnormal chloroplast development and the involvement of an alternative degradation pathway (pheophorbide *b* pathway). These findings provided insights into the molecular mechanism underlying the Chl *a/b* and leaf coloration in Chl *b*-deficient mutant of rice. However, the Chl *b* degradation in ch*11* is still unclear and needs further investigations to clarify.

Supplementary Materials: The following are available online at https://www.mdpi.com/article/10.3390/agriculture11050401/s1, Table S1: Primer sequences used for RT-qPCR in this study, Table S2: Summary of genome mapping, Table S3: Summary of gene mapping ratio.

Author Contributions: Conceptualization: C.-M.Y., M.K.N., H.C.N. and T.-H.S.; methodology: C.-M.Y., M.K.N., Z.-W.Y. and T.-H.S.; validation: M.K.N., S.-H.L., J.-W.L. and Z.-W.Y.; formal analysis: M.K.N. and T.-H.S.; investigation M.K.N., S.-H.L., J.-W.L. and Z.-W.Y.; writing: M.K.N. and H.C.N.; supervision: C.-M.Y.; project administration, M.K.N. and C.-M.Y. All authors have read and agreed to the published version of the manuscript.

Institutional Review Board Statement: Not applicable.

Informed Consent Statement: Not applicable.

Data Availability Statement: Not applicable.

Conflicts of Interest: The authors declare no conflict of interest.

References

1. Fageria, N.K. Yield physiology of rice. *J. Plant Nutr.* **2007**, *30*, 843–879. [CrossRef]
2. Xiong, Y.; Xie, Y.; Song, Q.; Zeng, W. The relationship between meteorological factors and rice yield in Liuzhi special zone. *Guizhou Agric. Sci.* **2009**, *10*, 79–81.
3. Liu, S.L.; Pu, C.; Ren, Y.X.; Zhao, X.L.; Zhao, X.; Chen, F.; Xiao, X.P.; Zhang, H.L. Yield variation of double-rice in response to climate change in Southern China. *Eur. J. Agron.* **2016**, *81*, 161–168. [CrossRef]
4. Li, J.; Yuan, J.C.; Cai, G.Z. Advances in the research of elevation on rice yield and quality. *Chin. Agric. Sci. Bull.* **2013**, *29*, 1–4.
5. Man, Y.; Wang, B.; Wang, J.; Slaný, M.; Yan, H.; Li, P.; El-Naggar, A.; Shaheen, S.M.; Rinklebe, J.; Feng, X. Use of biochar to reduce mercury accumulation in *Oryza sativa* L: A trial for sustainable management of historically polluted farmlands. *Environ. Int.* **2021**, *153*, 106527. [CrossRef]
6. Kruger, E.L.; Volin, J.C. Reexamining the empirical relation between plant growth and leaf photosynthesis. *Funct. Plant Biol.* **2006**, *33*, 421–429. [CrossRef] [PubMed]

7.   Makino, A. Photosynthesis, grain yield, and nitrogen utilization in rice and wheat. *Plant Physiol.* **2011**, *155*, 125–129. [CrossRef] [PubMed]

8.   Flood, P.J.; Kruijer, W.; Schnabel, S.K.; van der Schoor, R.; Jalink, H.; Snel, J.F.H.; Harbinson, J.; Aarts, M.G.M. Phenomics for photosynthesis, growth and reflectance in arabidopsis thaliana reveals circadian and long-term fluctuations in heritability. *Plant Methods* **2016**, *12*, 14. [CrossRef] [PubMed]

9.   Tanaka, A.; Tanaka, R. Chlorophyll metabolism. *Curr. Opin. Plant Biol.* **2006**, *9*, 248–255. [CrossRef] [PubMed]

10.   Wang, F.; Wang, G.; Li, X.; Huang, J.; Zheng, J. Heredity. physiology and mapping of a chlorophyll content gene of rice (*Oryza sativa* L.). *J. Plant Physiol.* **2008**, *165*, 324–330. [CrossRef]

11.   Kume, A.; Akitsu, T.; Nasahara, K.N. Why is chlorophyll *b* only used in light-harvesting systems? *J. Plant Res.* **2018**, *131*, 961–972. [CrossRef]

12.   Rühle, W.; Reiländer, H.; Otto, K.D.; Wild, A. Chlorophyll-protein-complexes of thylakoids of wild type and chlorophyll *b* mutants of *Arabidopsis thaliana*. *Photosynth. Res.* **1983**, *4*, 301–305. [CrossRef]

13.   Yang, C.M.; Osterman, J.C.; Markwell, J. Temperature sensitivity as a general phenomenon in a collection of chlorophyll-deficient mutants of sweetclover (*Melilotus alba*). *Biochem. Genet.* **1990**, *28*, 31–40. [CrossRef]

14.   Zhang, H.; Zhang, D.; Han, S.; Zhang, X.; Yu, D. Identification and gene mapping of a soybean chlorophyll-deficient mutant. *Plant Breed.* **2011**, *130*, 133–138. [CrossRef]

15.   Blankenship, R.E. *Molecular Mechanisms of Photosynthesis*; John Wiley & Sons: Hoboken, NJ, USA, 2014.

16.   Naqvi, K.R.; Melø, T.B.; Bangar Raju, B. Assaying the chromophore composition of photosynthetic systems by spectral reconstruction: Application to the light-harvesting complex (lhc ii) and the total pigment content of higher plants. *Spectrochim. Acta Part A Mol. Biomol. Spectrosc.* **1997**, *53*, 2229–2234. [CrossRef]

17.   Sager, J.C.; McFarlane, J.C. *Radiation-Plant Growth Chamber Handbook*; Iowa State University of Science and Technology: Ames, IA, USA, 1997; pp. 1–29.

18.   Landi, M.; Zivcak, M.; Sytar, O.; Brestic, M.; Allakhverdiev, S.I. Plasticity of photosynthetic processes and the accumulation of secondary metabolites in plants in response to monochromatic light environments: A review. *Biochim. Biophys. Acta Bioenerg.* **2020**, *1861*, 148131. [CrossRef] [PubMed]

19.   Ito, H.; Ohtsuka, T.; Tanaka, A. Conversion of chlorophyll *b* to chlorophyll *a* via 7-hydroxymethyl chlorophyll. *J. Biol. Chem.* **1996**, *271*, 1475–1479. [CrossRef]

20.   Gupta, J. Climate Change and Water Law. In *Impact of Climate Change on Water and Health*; CRC Press: Boca Raton, FL, USA, 2013.

21.   Avenson, T.J.; Cruz, J.A.; Kanazawa, A.; Kramer, D.M. Regulating the proton budget of higher plant photosynthesis. *Proc. Natl. Acad. Sci. USA* **2005**, *102*, 9709–9713. [CrossRef]

22.   Mitchell, P.L.; Sheehy, J.E. Supercharging rice photosynthesis to increase yield. *New Phytol.* **2006**, *171*, 688–693. [CrossRef]

23.   Huang, J.; Qin, F.; Zang, G.; Kang, Z.; Zou, H.; Hu, F.; Yue, C.; Li, X.; Wang, G. Mutation of OSDET1 increases chlorophyll content in rice. *Plant Sci.* **2013**, *210*, 241–249. [CrossRef] [PubMed]

24.   Masuda, T.; Fujita, Y. Regulation and evolution of chlorophyll metabolism. *Photochem. Photobiol. Sci.* **2008**, *7*, 1131–1149. [CrossRef]

25.   Lai, Y.C.; Wang, S.Y.; Gao, H.Y.; Nguyen, K.M.; Nguyen, C.H.; Shih, M.C.; Lin, K.H. Physicochemical properties of starches and expression and activity of starch biosynthesis-related genes in sweet potatoes. *Food Chem.* **2016**, *199*, 556–564. [CrossRef] [PubMed]

26.   Nguyen, M.K.; Shih, T.H.; Lin, S.H.; Huang, W.D.; Yang, C.M. Transcription analysis of chlorophyll biosynthesis in wildtype and chlorophyll *b*-lacking rice (*Oryza sativa* L.). *Photosynthetica* **2020**, *58*, 702–711. [CrossRef]

27.   Albrecht, V.; Ingenfeld, A.; Apel, K. Characterization of the snowy cotyledon 1 mutant of *Arabidopsis thaliana*: The impact of chloroplast elongation factor g on chloroplast development and plant vitality. *Plant Mol. Biol.* **2006**, *60*, 507–518. [CrossRef] [PubMed]

28.   Pogson, B.J.; Ganguly, D.; Albrecht-Borth, V. Insights into chloroplast biogenesis and development. *Biochim. Biophys. Acta Bioenerg.* **2015**, *1847*, 1017–1024. [CrossRef] [PubMed]

29.   Abe, T.; Matsuyama, T.; Sekido, S.; Yamaguchi, I.; Yoshida, S.; Kameya, T. Chlorophyll-deficient mutants of rice demonstrated the deletion of a DNA fragment by heavy-ion irradiation. *J. Radiat. Res.* **2002**, *43*, S157–S161. [CrossRef] [PubMed]

30.   Cha, K.W.; Lee, Y.J.; Koh, H.J.; Lee, B.M.; Nam, Y.W.; Paek, N.C. Isolation, characterization, and mapping of the stay green mutant in rice. *Theor. Appl. Genet.* **2002**, *104*, 526–532. [CrossRef] [PubMed]

31.   Jung, K.H.; Hur, J.; Ryu, C.H.; Choi, Y.; Chung, Y.Y.; Miyao, A.; Hirochika, H.; An, G. Characterization of a rice chlorophyll-deficient mutant using the T-DNA gene-trap system. *Plant Cell Physiol.* **2003**, *44*, 463–472. [CrossRef]

32.   Chen, X.; Zhang, W.; Xie, Y.; Lu, W.; Zhang, R. Comparative proteomics of thylakoid membrane from a chlorophyll *b*-less rice mutant and its wild type. *Plant Sci.* **2007**, *173*, 397–407. [CrossRef]

33.   Chu, P.; Yan, G.X.; Yang, Q.; Zhai, L.N.; Zhang, C.; Zhang, F.Q.; Guan, R.Z. ITRAQ-based quantitative proteomics analysis of brassica napus leaves reveals pathways associated with chlorophyll deficiency. *J. Proteom.* **2015**, *113*, 244–259. [CrossRef]

34.   Zhu, H.; Zhou, Y.Y.; Zhai, H.; He, S.Z.; Zhao, N.; LIU, Q.Q.C. Transcriptome profiling reveals insights into the molecular mechanism of drought tolerance in sweetpotato. *J. Integr. Agric.* **2019**, *18*, 9–23. [CrossRef]

35.   Vothknecht, U.C.; Kannangara, C.G.; Von Wettstein, D. Expression of catalytically active barley glutamyl tRNAglu reductase in *escherichia coli* as a fusion protein with glutathione s-transferase. *Proc. Natl. Acad. Sci. USA* **1996**, *93*, 9287–9291. [CrossRef]

36. Harpster, M.H.; Mayfield, S.P.; Taylor, W.C. Effects of pigment-deficient mutants on the accumulation of photosynthetic proteins in maize. *Plant Mol. Biol.* **1984**, *3*, 59–71. [CrossRef] [PubMed]

37. Droppa, M.; Ghirardi, M.L.; Horvath, G.; Melis, A. Chlorophyll *b* deficiency in soybean mutants. II. thylakoid membrane development and differentiation. *BBA Bioenerg.* **1988**, *932*, 138–145. [CrossRef]

38. Zhao, H.B.; Guo, H.J.; Zhao, L.S.; Gu, J.Y.; Zhao, S.R.; Li, J.H.; Liu, L.X. Agronomic traits and photosynthetic characteristics of chlorophyll-deficient wheat mutant induced by spaceflight environment. *Acta Agron. Sin.* **2011**, *37*, 119–126.

39. Somerville, C.R. Analysis of photosynthesis with mutants of higher plants and algae. *Annu. Rev. Plant Physiol.* **1986**, *37*, 467–506. [CrossRef]

40. Terao, T.; Yamashita, A.; Katoh, S. Chlorophyll *b*-deficient mutants of rice: II. antenna chlorophyll *a/b*-proteins of photosystem I and II. *Plant Cell Physiol.* **1985**, *26*, 1369–1377.

41. Terao, T.; Yamashita, A.; Katoh, S. Chlorophyll *b*-deficient mutants of rice. 1. Absorption and fluorescence spectra and chlorophyll *a/b* ratios. *Plant Cell Physiol.* **1985**, *26*, 1361–1367.

42. Terao, T.; Sonoike, K.; Yamazaki, J.; Kamimura, Y.; Katoh, S. Stoichiometries of photosystem I and photosystem II in rice mutants differently deficient in chlorophyll *b*. *Plant Cell Physiol.* **1996**, *37*, 299–306. [CrossRef]

43. Yang, C.M.; Chang, K.W.; Yin, M.H.; Huang, H.M. Methods for the determination of the chlorophylls and their derivatives. *Taiwania* **1998**, *43*, 116–122.

44. Spurr, A.R. A low-viscosity epoxy resin embedding medium for electron microscopy. *J. Ultrastruct. Res.* **1969**, *26*, 31–43. [CrossRef]

45. Audic, S.; Claverie, J.M. The significance of digital gene expression profiles. *Genome Res.* **1997**, *7*, 986–995. [CrossRef]

46. Livak, K.J.; Schmittgen, T.D. Analysis of relative gene expression data using real-time quantitative PCR and the $2^{-\Delta\Delta ct}$ method. *Methods* **2001**, *25*, 402–408. [CrossRef] [PubMed]

47. Bujaldon, S.; Kodama, N.; Rappaport, F.; Subramanyam, R.; de Vitry, C.; Takahashi, Y.; Wollman, F.A. Functional accumulation of antenna proteins in chlorophyll *b*-less mutants of *Chlamydomonas reinhardtii*. *Mol. Plant* **2017**, *10*, 115–130. [CrossRef] [PubMed]

48. Liu, X.; Sun, L.; Wu, Q.; Men, X.; Yao, L.; Xing, S. Transcriptome profile analysis reveals the ontogenesis of rooted chichi in *Ginkgo biloba* L. *Gene* **2018**, *669*, 8–14. [CrossRef]

49. Yang, Y.; Chen, X.; Xu, B.; Li, Y.; Ma, Y.; Wang, G. Phenotype and transcriptome analysis reveals chloroplast development and pigment biosynthesis together influenced the leaf color formation in mutants of *Anthurium andraeanum* 'sonate'. *Front. Plant Sci.* **2015**, *6*, 139. [CrossRef] [PubMed]

50. Yamazaki, J. Changes in the photosynthetic characteristics and photosystem stoichiometries in wild-type and Chl *b*-deficient mutant rice seedlings under various irradiances. *Photosynthetica* **2010**, *48*, 521–529. [CrossRef]

51. Rüdiger, W. Chlorophyll metabolism: From outer space down to the molecular level. *Phytochemistry* **1997**, *46*, 1151–1167. [CrossRef]

52. Liu, W.; Fu, Y.; Hu, G.; Si, H.; Zhu, L.; Wu, C.; Sun, Z. Identification and fine mapping of a thermo-sensitive chlorophyll deficient mutant in rice (*Oryza sativa* L.). *Planta* **2007**, *226*, 785–795. [CrossRef]

53. Liu, X.; Li, L.; Li, M.; Su, L.; Lian, S.; Zhang, B.; Li, X.; Ge, K.; Li, L. AhGLK1 Affects chlorophyll biosynthesis and photosynthesis in peanut leaves during recovery from drought. *Sci. Rep.* **2018**, *8*, 2250. [CrossRef]

54. Yang, H.Y.; Xia, X.W.; Fang, W.; Fu, Y.; An, M.M.; Zhou, M.B. Identification of genes involved in spontaneous leaf color variation in *Pseudosasa japonica*. *Genet. Mol. Res.* **2015**, *14*, 11827–11840. [CrossRef]

55. Li, Y.; He, N.; Hou, J.; Xu, L.; Liu, C.; Zhang, J.; Wang, Q.; Zhang, X.; Wu, X. Factors influencing leaf chlorophyll content in natural forests at the biome scale. *Front. Ecol. Evol.* **2018**, *6*, 64. [CrossRef]

56. Wu, Z.M.; Zhang, X.; Wang, J.L.; Wan, J.M. Leaf chloroplast ultrastructure and photosynthetic properties of a chlorophyll-deficient mutant of rice. *Photosynthetica* **2014**, *52*, 217–222. [CrossRef]

57. Seo, T.S.; Bai, X.; Ruparel, H.; Li, Z.; Turro, N.J.; Ju, J. Photocleavable fluorescent nucleotides for dna sequencing on a chip constructed by site-specific coupling chemistry. *Proc. Natl. Acad. Sci. USA* **2004**, *101*, 5488–5493. [CrossRef]

58. Wang, Z.; Gerstein, M.; Snyder, M. RNA-Seq: A revolutionary tool for transcriptomics. *Nat. Rev. Genet.* **2009**, *10*, 57. [CrossRef] [PubMed]

59. Li, Y.; Zhang, Z.; Wang, P.; Wang, S.; Ma, L.; Li, L.; Yang, R.; Ma, Y.; Wang, Q. Comprehensive transcriptome analysis discovers novel candidate genes related to leaf color in a lagerstroemia indica yellow leaf mutant. *Genes Genom.* **2015**, *37*, 851–863. [CrossRef]

60. Schmitz, A.J.; Glynn, J.M.; Olson, B.J.; Stokes, K.D.; Osteryoung, K.W. *Arabidopsis* FtsZ2-1 and FtsZ2-2 are functionally redundant, but FtsZ-based plastid division is not essential for chloroplast partitioning or plant growth and development. *Mol. Plant* **2009**, *2*, 1211–1222. [CrossRef] [PubMed]

61. Swid, N.; Nevo, R.; Kiss, V.; Kapon, R.; Dagan, S.; Snir, O.; Adam, Z.; Falconet, D.; Reich, Z.; Charuvi, D. Differential impacts of FtsZ proteins on plastid division in the shoot apex of *Arabidopsis*. *Dev. Biol.* **2018**, *441*, 83–94. [CrossRef]

62. Goral, T.K.; Johnson, M.P.; Duffy, C.D.; Brain, A.P.R.; Ruban, A.V.; Mullineaux, C.W. Light-harvesting antenna composition controls the macrostructure and dynamics of thylakoid membranes in *Arabidopsis*. *Plant J.* **2012**, *69*, 289–301. [CrossRef]

63. Zhao, X.; Chen, T.; Feng, B.; Zhang, C.; Peng, S.; Zhang, X.; Fu, G.; Tao, L. Non-photochemical quenching plays a key role in light acclimation of rice plants differing in leaf color. *Front. Plant Sci.* **2017**, *7*, 1968. [CrossRef] [PubMed]

64. Shi, L.X.; Hall, M.; Funk, C.; Schröder, W.P. Photosystem ii, a growing complex: Updates on newly discovered components and low molecular mass proteins. *Biochim. Biophys. Acta Bioenerg.* **2012**, *1817*, 13–25. [CrossRef] [PubMed]

65. Amarnath, K.; Bennett, D.I.G.; Schneider, A.R.; Fleming, G.R. Multiscale model of light harvesting by photosystem II in plants. *Proc. Natl. Acad. Sci. USA* **2016**, *113*, 1156–1161. [CrossRef]
66. Bennett, J. Protein phosphorylation in green plant chloroplasts. *Annu. Rev. Plant Biol.* **1991**, *42*, 281–311. [CrossRef]
67. Allen, J.F. How does protein phosphorylation regulate photosynthesis? *Trends Biochem. Sci.* **1992**, *17*, 12–17. [CrossRef]
68. Standfuss, J.; Terwisscha van Scheltinga, A.C.; Lamborghini, M.; Kühlbrandt, W. Mechanisms of photoprotection and nonphotochemical quenching in pea light-harvesting complex at 2.5 Å resolution. *EMBO J.* **2005**, *24*, 919–928. [CrossRef]
69. Yang, C.M.; Chen, H.Y. Grana stacking is normal in a chlorophyll-deficient LT8 mutant of rice. *Bot. Bull. Acad. Sin.* **1996**, *37*, 31–34.
70. Jenny, A.; Mark, W.; Robin, G.W.; Caroline, A.H.; Alexander, V.R.; Peter, H.; Stefan, J. Absence of the Lhcb1 and Lhcb2 proteins of the light-harvesting complex of photosystem II–effects on photosynthesis, grana stacking and fitness. *Plant J.* **2003**, *35*, 350–361. [CrossRef]
71. Kim, E.H.; Li, X.P.; Razeghifard, R.; Anderson, J.M.; Niyogi, K.K.; Pogson, B.J.; Chow, W.S. The multiple roles of light-harvesting chlorophyll a/b-protein complexes define structure and optimize function of *Arabidopsis* chloroplasts: A study using two chlorophyll *b*-less mutants. *Biochim. Biophys. Acta Bioenerg.* **2009**, *1787*, 973–984. [CrossRef]
72. Tyutereva, E.; Ivanova, A.; Voitsekhovskaja, O. On the role of chlorophyll *b* in ontogenetic adaptations of plants. *Biol. Bull. Rev.* **2014**, *4*, 507–514. [CrossRef]
73. Barber, J. Influence of surface charges on thylakoid structure and function. *Annu. Rev. Plant Physiol.* **1982**, *33*, 261–295. [CrossRef]
74. Mulo, P. Chloroplast-targeted ferredoxin-nadp+ oxidoreductase (fnr): Structure, function and location. *Biochim. Biophys. Acta Bioenerg.* **2011**, *1807*, 927–934. [CrossRef]
75. Fromme, P.; Melkozernov, A.; Jordan, P.; Krauss, N. Sstructure and function of photosystem I: Interaction with its soluble electron carriers and external antenna systems. *FEBS Lett.* **2003**, *555*, 40–44. [CrossRef]
76. Nelson, N.; Yocum, C.F. Structure and function of photosystems I and II. *Annu. Rev. Plant Biol.* **2006**, *57*, 521–565. [CrossRef]
77. Voitsekhovskaja, O.V.; Tyutereva, E.V. Chlorophyll *b* in angiosperms: Functions in photosynthesis, signaling and ontogenetic regulation. *J. Plant Physiol.* **2015**, *189*, 51–64. [CrossRef]
78. Fang, Y.; Zhao, S.; Zhang, F.; Zhao, A.; Zhang, W.; Zhang, M.; Liu, L. The *Arabidopsis* glutamyl-tRNA reductase (*GLUTR*) forms a ternary complex with flu and *GLUTR*-binding protein. *Sci. Rep.* **2016**, *6*, 19756. [CrossRef]
79. Sheng, Z.; Lv, Y.; Li, W.; Luo, R.; Wei, X.; Xie, L.; Jiao, G.; Shao, G.; Wang, J.; Tang, S.; et al. Yellow-leaf 1 encodes a magnesium-protoporphyrin ix monomethyl ester cyclase, involved in chlorophyll biosynthesis in rice (*Oryza sativa* L.). *PLoS ONE* **2017**, *12*, e0177989. [CrossRef]
80. Nomata, J.; Swem, L.R.; Bauer, C.E.; Fujita, Y. Overexpression and characterization of dark-operative protochlorophyllide reductase from *Rhodobacter capsulatus*. *Biochim. Biophys. Acta Bioenerg.* **2005**, *1708*, 229–237. [CrossRef]
81. Fujita, Y. Protochlorophyllide reduction: A key step in the greening of plants. *Plant Cell Physiol.* **1996**, *37*, 411–421. [CrossRef] [PubMed]
82. Apel, K. Chlorophyll biosynthesis—Metabolism and strategies of higher plants to avoid photooxidative stress. In *Regulation of Photosynthesis*; Springer: Berlin/Heidelberg, Germany, 2001; pp. 235–252.
83. Schoefs, B. The protochlorophyllide–chlorophyllide cycle. *Photosynth. Res.* **2001**, *70*, 257–271. [CrossRef] [PubMed]
84. Shimoda, Y.; Ito, H.; Tanaka, A. Conversion of chlorophyll *b* to chlorophyll *a* precedes magnesium dechelation for protection against necrosis in *Arabidopsis*. *Plant J.* **2012**, *72*, 501–511. [CrossRef] [PubMed]
85. Tanaka, A.; Tanaka, R. The biochemistry, physiology, and evolution of the chlorophyll cycle. In *Advances in Botanical Research*; Elsevier: Amsterdam, The Netherlands, 2019.